CHAPTER 3

Derivation of Moment Invariants

Huazhong Shu, Limin Luo and Jean Louis Coatrieux

In most computer vision applications, the extraction of key image features, whatever the transformations applied and the image degradations observed, is of major importance. A large diversity of approaches has been reported in the literature. This chapter concentrates on one particular processing frame: the moment-based methods. It provides a survey of methods proposed so far for the derivation of moment invariants to geometric transforms and blurring effects. Theoretical formulations and some selected examples dealing with very different problems are given.

Huazhong Shu, Limin Luo
Laboratory of Image Science and Technology, School of Computer Science and Engineering,
Southeast University, 210096 Nanjing, China
Centre de Recherche en Information Biomédicale Sino-français (CRIBs), France
e-mail: shu.list@seu.edu.cn

Jean Louis Coatrieux
Laboratory of Image Science and Technology, School of Computer Science and Engineering,
Southeast University, 210096 Nanjing, China
INSERM U642, 35042 Rennes, France
Laboratoire Traitement du Signal et de l'Image, Université de Rennes I, 35042 Rennes, France
Centre de Recherche en Information Biomédicale Sino-français (CRIBs), France
e-mail: jean-louis.coatrieux@univ-rennes1.fr

Editor: G.A. Papakostas, *Moments and Moment Invariants - Theory and Applications*
DOI: 10.15579/gcsr.vol1.ch3, GCSR Vol. 1,

3.1 Introduction

Nowadays, gray level and color images play a central role in many research fields going from biology, medicine, chemistry, physics up to archeology, geology and others. In the sole engineering area, to take a few examples, robot control, remote sensing, road traffic analysis, enhanced virtual reality, compression and watermarking are concerned. All these fields required tools for extracting, quantifying and interpreting the information they convey. Such tools and methods refer to image processing or computer vision at large.

They can be classified in a general way according to low-level methods (bottom-up approaches operating on edges or regions) or high-level techniques (top-down approaches driven by models of objects and scenes). These image analyses depend on the applications to face. Image acquisition is a first and critical step determining the quality of the input data and therefore the performance of the analysis that will be carried out. A number of different physics are available to get the observations required: for instance optical (including infrared camera), X-ray and acoustic sensors. Specific procedures must be designed to generate 2D and 3D images before considering any analysis: a good example is found with Computer Tomography (CT Scanner) in medicine, where reconstruction from projection data has to be performed first.

Then, and depending on the nature of the data and the targets, key steps should be addressed among which object boundary detection, object segmentation, matching and registration, pattern recognition, shape modeling, texture labeling, motion tracking, classification, etc. Even if major progresses have been recognized over the past decades by the emergence of very diverse methodological frames (for instance, level-set and graph-cut techniques aimed at object segmentation), significant difficulties remain when the images are too noisy or degraded, the object contrasts too low, when we have to face to deformable objects or to important occlusions.

In this very dense landscape of methods and problems [34, 23], the description of object invariants for point-of-interest detection and matching, registration, image forgery detection, image indexing-retrieval and more widely for pattern recognition, is of high significance. They first have to deal with geometric transformations such as translation, scale and rotation, and more generally to affine transformation. Image blurring is another major concern. Blur may occur due to wrong focus, object/camera motion. The performance of any computer vision system, whatever their target application, relies on the specific feature extraction technique used.

A popular class of invariant features is based on the moment techniques. As noted by Ghorbel et al. [5, 14], the most important properties to assess by the image descriptors are: (1) invariance against some geometrical transformations; (2) stability to noise, to blur, to non-rigid and small local deformations; and (3) completeness. The objective of this chapter is to present a comprehensive survey of the state-of-the-art on the moment invariants to geometric transformations and to blur in pattern recognition. Proofs of theorems are referred to already published papers. Some illustrations on different applications will be also provided along the chapter.

3.2 Derivation of Moment Invariants to Geometric Transformations

In the past decades, the construction of moment invariants and their application to pattern recognition have been extensively investigated. They can be classified into three categories: (1) Normalization techniques [17, 21]; (2) Indirect methods [20, 11]; (3) Direct approaches. It is well known that the normalization process can be used to achieve the invariance. However, such a process may lead to inaccuracy since the normalization of the images requires re-sampling and re-quantifying. The indirect methods make use of geometric moments or complex moments to achieve the invariance, but they are time expensive due to the long time allocated to compute the polynomial coefficients when orthogonal moments are concerned. In order to improve the accuracy and to speed up the computational efficiency, many direct algorithms have been reported in the literature. Chong et al. [3] proposed a method based on the properties of pseudo-Zernike polynomial to derive the scale invariants of pseudo-Zernike moments. A similar approach was then used to construct both translation and scale invariants of Legendre moments [4]. The problem of scale and translation invariants of Tchebichef moments has been investigated by Zhu et al. [43]. Discrete orthogonal moments such as Tchebichef moments yield better performance than the continuous orthogonal moments, but the rotation invariants are difficult to derive. To overcome this shortcoming, Mukundan [19] introduced the radial Tchebichef moments, which are defined in polar coordinate system, to achieve the rotation invariance. It was shown that the methods reported in [3, 4, 43, 19] perform better than the classical approaches such as image normalization and indirect methods. However, it seems difficult to obtain the completeness property by the above mentioned methods since no explicit formulation is derived for moment invariants.

A set of invariant descriptors is said to be complete if it satisfies the following property: two objects have the same shape if and only if they have the same set of invariants. A number of studies have been conducted on completeness. Flusser et al. proposed a complete set of rotation invariants by normalizing the complex moments [6, 7]. The construction of a complete set of similarity (translation, scale and rotation) invariant descriptors by means of some linear combinations of complex moments has been addressed by Ghorbel et al. [14].

This first part of the chapter will review the ways to construct a complete set of orthogonal moments defined in polar coordinate system, and how to derive a set of moment invariants with respect to affine transformation.

3.2.1 Derivation of a Complete Set of Orthogonal Fourier–Mellin Moment Invariants

It is well known that the moments defined in polar coordinate system including the complex moments, Zernike moments, pseudo-Zernike moments [24], orthogonal Fourier-Mellin moments [28], Bessel–Fourier moments [36], can easily achieve the rotation invariance by taking the module of the moments. However, the moment magnitudes do not generate a complete set of invariants. In this section, we present a general

scheme to derive a complete set of radial orthogonal moments with respect to similarity transformation. We take the orthogonal Fourier–Mellin moments (OFMMs) as an example for illustration [39].

The 2D OFMM, Z_{pq}^{f}, of order p with repetition q of an image intensity function $f(r,\theta)$ is defined as [28]

$$Z_{pq}^{f}=\frac{p+1}{\pi}\int_{0}^{2\pi}\int_{0}^{1}Q_{p}(r)\,e^{-jq\theta}f(r,\theta)\,rdrd\theta,\quad |q|\leq p, \tag{3.1}$$

where $Q_p(r)$ is a set of radial polynomials given by

$$Q_{p}(r)=\sum_{k=0}^{p}c_{p,k}r^{k}, \tag{3.2}$$

with

$$c_{p,k}=(-1)^{p+k}\,\frac{(p+k+1)!}{(p-k)!k!\,(k+1)!} \tag{3.3}$$

Since OFMMs are defined in terms of polar coordinates (r,θ) with $|r|\leq 1$, the computation of OFMMs requires a linear transformation of the image coordinates to a suitable domain inside a unit circle. Here, we use the mapping transformation proposed by Chong et al. [3], which is shown in Fig.(3.1). Based on this transformation, we have the following discrete approximation of Eq.(3.1):

$$Z_{pq}^{f}=\frac{p+1}{\pi}\sum_{i=0}^{N-1}\sum_{j=0}^{N-1}Q_{p}(r_{ij})\,e^{-jq\theta_{ij}}f(i,j), \tag{3.4}$$

where the image coordinate transformation to the interior of the unit circle is given by

$$r_{ij}=\sqrt{(c_1 i+c_2)^2+(c_1 j+c_2)^2},\quad \theta_{ij}=\tan^{-1}\left(\frac{c_1 j+c_2}{c_1 i+c_2}\right) \tag{3.5}$$

with $c_1=\frac{\sqrt{2}}{N-1}$, $c_2=\frac{1}{\sqrt{2}}$.

We now describe a general approach to derive a complete set of OFMM invariants. We use the same method to achieve the translation invariance as described in [14]. That is, the origin of the coordinate system is located at the center of mass of the object to achieve the translation invariance. This center of mass, (x_c,y_c), can be computed from the first geometric moments of the object as follows

$$x_c=\frac{m_{10}^{f}}{m_{00}^{f}},\quad y_c=\frac{m_{01}^{f}}{m_{00}^{f}}, \tag{3.6}$$

where $m_{pq}^{f}$are the $(p+q)$-th order geometric moments defined by

$$m_{pq}^{f}=\int_{-\infty}^{\infty}\int_{-\infty}^{\infty}x^{p}y^{q}f(x,y)\,dxdy. \tag{3.7}$$

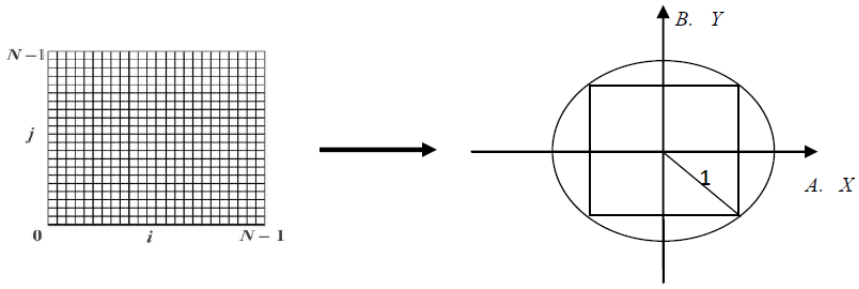

Figure 3.1: Mapping image inside the unit circle.

Let $U_m(r) = (Q_0(r), Q_1(r), ..., Q_m(r))^T$ and $M_m(r) = \left(r^0, r^1, ..., r^m\right)^T$ be two vectors, where the superscript T indicates the transposition, we have

$$U_m(r) = C_m M_m(r), \tag{3.8}$$

where $C_m = (c_{i,j})$, with $0 \leq j \leq i \leq m$, is a $(m+1) \times (m+1)$ lower triangular matrix whose element $c_{i,j}$ is given by Eq.(3.3).

Since all the diagonal elements of C_m, $c_{l,l} = \frac{(2l+1)!}{l!(l+1)!}$, are not zero, the matrix C_m is non-singular, thus

$$M_m(r) = (C_m)^{-1} U_m(r) = D_m U_m(r), \tag{3.9}$$

where $D_m = (d_{i,,j})$, with $0 \leq j \leq i \leq m$, is the inverse matrix of C_m. It is also a $(m+1) \times (m+1)$ lower triangular matrix. The computation of the elements of D_m is given in the following Proposition.

Proposition 1. *For the lower triangular matrix C_m whose elements $c_{i,j}$ are defined by Eq.(3.3), the elements of the inverse matrix D_m are given by*

$$d_{i,j} = \frac{(2j+2)\, i!\, (i+1)!}{(i+1)!\, (i+j+2)!}. \tag{3.10}$$

The proof of Proposition 1 can be found in [39].

Let f and g be two images display the same pattern but with distinct orientation β and scale λ, i.e., $g(r,\theta) = f(r/\lambda, \theta - \beta)$. The OFMM of the image intensity function $g(r,\theta)$ is defined as

$$\begin{aligned} Z_{pq}^g &= \frac{p+1}{\pi} \int_0^{2\pi} \int_0^1 Q_p(r)\, e^{-jq\theta} g(r,\theta)\, r dr d\theta \\ &= \lambda^2 e^{-jq\beta} \frac{p+1}{\pi} \int_0^{2\pi} \int_0^1 Q_p(\lambda r)\, e^{-jq\theta} f(r,\theta)\, r dr d\theta, \end{aligned} \tag{3.11}$$

Letting

$$U_m(\lambda r) = (Q_0(\lambda r), Q_1(\lambda r), ..., Q_m(\lambda r))^T,$$
$$M_m(\lambda r) = \left(1, (\lambda r)^1, ..., (\lambda r)^m\right)^T,$$

it can be seen from Eq.(3.8) that

$$U_m(\lambda r) = C_m M_m(\lambda r). \tag{3.12}$$

On the other hand,

$$\begin{aligned} M_m(\lambda r) &= diag\left(1, \lambda^1, ..., \lambda^m\right)\left(1, r^1, ..., r^m\right)^T \\ &= diag\left(1, \lambda^1, ..., \lambda^m\right) M_m(r). \end{aligned} \tag{3.13}$$

Substituting Eq.(3.13) and Eq.(3.9) into Eq.(3.12), we obtain

$$U_m(\lambda r) = C_m diag\left(1, \lambda^1, ..., \lambda^m\right) D_m U_m(r). \tag{3.14}$$

By expanding Eq.(3.14), we have

$$Q_p(\lambda r) = \sum_{k=0}^{p} Q_k(r) \sum_{l=k}^{p} \lambda^l c_{p,l} d_{l,k}. \tag{3.15}$$

With the help of Eq.(3.15), Eq.(3.11) can be rewritten as

$$\begin{aligned} Z_{pq}^g &= \lambda^2 e^{-jq\beta} \frac{p+1}{\pi} \int_0^{2\pi} \int_0^1 Q_p(\lambda r) e^{-jq\theta} f(r,\theta) r dr d\theta \\ &= \lambda^2 e^{-jq\beta} \frac{p+1}{\pi} \int_0^{2\pi} \int_0^1 \left(\sum_{k=0}^{p} Q_k(r) \sum_{l=k}^{p} \lambda^l c_{p,l} d_{l,k} \right) e^{-jq\theta} f(r,\theta) r dr d\theta \\ &= e^{-jq\beta} \sum_{k=0}^{p} \frac{p+1}{k+1} \times \frac{k+1}{\pi} \sum_{l=k}^{p} \lambda^l c_{p,l} d_{l,k} \int_0^{2\pi} \int_0^1 Q_k(r) e^{-jq\theta} f(r,\theta) r dr d\theta \\ &= e^{-jq\beta} \sum_{k=0}^{p} \frac{p+1}{k+1} \left(\sum_{l=k}^{p} \lambda^{l+2} c_{p,l} d_{l,k} \right) Z_{pq}^f. \end{aligned} \tag{3.16}$$

The above equation shows that the 2D scaled and rotated OFMMs, Z_{pq}^g, can be expressed as a linear combination of the original OFMMs Z_{pq}^f with $0 \le k \le p$. By using this relationship, we can construct a complete set of both rotation and scale invariants I_{pq}^f, which is described in the following theorem.

Theorem 1. *For a given integer q and any positive integer p , let*

$$I_{pq}^{f}=\sum_{k=0}^{p}e^{-jq\theta_f}\frac{p+1}{k+1}\left(\sum_{l=k}^{p}\Gamma_{f}^{-(l+2)}c_{p,l}d_{l,k}\right)Z_{pq}^{f}, \tag{3.17}$$

with $\theta_f=\arg\left(Z_{11}^{f}\right)$ and $\Gamma_f=\sqrt{Z_{00}^{f}}$. Then I_{pq}^{f}, is invariant to both image rotation and scaling.

The reader can refer to [39]for the proof of Theorem 1.

Equation 3.17 can be expressed in matrix form as

$$\begin{aligned}\begin{pmatrix} I_{0q}^{f}\\ I_{1q}^{f}\\ .\\ .\\ .\\ I_{pq}^{f}\end{pmatrix} =&e^{-jq\theta_f}diag\left(1,2,...,p+1\right)C_p diag\left(\Gamma_f^{-2},\Gamma_f^{-3},...,\Gamma_f^{-(p+2)}\right)\times\\ &D_p diag\left(1,\frac{1}{2},...,\frac{1}{p+1}\right)\begin{pmatrix} Z_{0q}^{f}\\ Z_{1q}^{f}\\ .\\ .\\ .\\ Z_{pq}^{f}\end{pmatrix}.\end{aligned} \tag{3.18}$$

It is easy to verify that the set of invariants is complete by rewriting Eq.(3.18) as

$$\begin{aligned}\begin{pmatrix} Z_{0q}^{f}\\ Z_{1q}^{f}\\ .\\ .\\ .\\ Z_{pq}^{f}\end{pmatrix} =&e^{jq\theta_f}diag\left(1,2,...,p+1\right)C_p diag\left(\Gamma_f^{2},\Gamma_f^{3},...,\Gamma_f^{(p+2)}\right)\times\\ &D_p diag\left(1,\frac{1}{2},...,\frac{1}{p+1}\right)\begin{pmatrix} I_{0q}^{f}\\ I_{1q}^{f}\\ .\\ .\\ .\\ I_{pq}^{f}\end{pmatrix}.\end{aligned} \tag{3.19}$$

Thus, we have

$$Z_{pq}^{f}=\sum_{k=0}^{p}e^{jq\theta_f}\frac{p+1}{k+1}\left(\sum_{l=k}^{p}\Gamma_{f}^{(l+2)}c_{p,l}d_{l,k}\right)I_{pq}^{f}. \tag{3.20}$$

The above equation shows that the set of invariants is complete. Note that the above approach is general enough to be extended to any other radial orthogonal moments. The only difference is that for a given matrix C_p whose elements correspond to the coefficients of a set of radial polynomials up to order p, we need to find its inverse matrix, D_p.

3.2.2 Derivation of Affine Invariants by Orthogonal Legendre Moments

Affine moment invariants (AMIs) are useful features of an image since they are invariant to general linear transformations of an image. The AMIs were introduced independently by Reiss [25] and Flusser and Suk [9]. Since then, they have been utilized as pattern features in a number of applications such as pattern recognition, pattern matching, image registration and contour shape estimation.

The construction of affine moment invariants has been also extensively investigated. The existing methods can be generally classified into two categories: (1) direct method, and (2) image normalization. Among the direct methods, Reiss [25] and Flusser and Suk [9] derived the AMIs based on the theory of algebraic invariants and tensor techniques. Suk and Flusser [32] used a graph method to construct the affine moment invariants. Liu et al. [18] proposed an automatic method for generating the affine invariants. Normalization is an alternative approach to derive the moment invariants. An affine normalization approach was first introduced by Rothe et al. [26]. In their work, two different affine decompositions were used. The first known as XSR decomposition consists of two skews, anisotropic scaling and rotation. The second is the XYS and consists of two skews and anisotropic scaling. Zhang et al. [41] performed a study of these affine decompositions and pointed out that both decompositions lead to some ambiguities. More details on these decompositions will be given below. Pei and Lin [22] presented an affine normalization for asymmetrical object and Suk and Flusser [33] dealt with symmetrical object. Zhang and Wu [40] extended the method to Legendre moments. Shen and Ip [27] used the generalized complex moments and analyzed their behavior in recognition of symmetrical objects.

Almost all the existing methods to derive the affine invariants are based on geometric moments and complex moments. Since the kernel functions of both geometric moments and complex moments are not orthogonal, this leads to information redundancy when they are used to represent the image. This motivates us to use the orthogonal moments in the construction of affine moment invariants. We present here a new method to derive a set of affine invariants based on the orthogonal Legendre moments.

The 2D $(p+q)$-th order Legendre moment of an image function $f(x,y)$ is defined as [35]

$$L_{pq}^{(f)} = \int_{-1}^{1}\int_{-1}^{1} P_p(x)\, P_q(x)\, f(x,y)\, dxdy,\ \ p,q = 0,1,2,\ldots, \tag{3.21}$$

where $P_p(x)$ is the p-th order orthonormal Legendre polynomials given by

$$P_p(x) = \sum_{k=0}^{p} c_{p,k} x^k, \tag{3.22}$$

with

$$c_{p,k} = \begin{cases} \sqrt{\frac{2p+1}{2}} \frac{(-1)^{\frac{p-k}{2}}(p+k)!}{2^p \left(\frac{p-k}{2}\right)! \left(\frac{p+k}{2}\right)! k!}, & p-k = even \\ 0, & p-k-odd \end{cases}. \tag{3.23}$$

It can be deduced from Eq.(3.22) that

$$x^p = \sum_{k=0}^{p} d_{p,k} P_k(x), \tag{3.24}$$

where $D_M = (d_{p,k})$, $0 \le k \le p \le M$, is the inverse matrix of the lower triangular matrix $C_M = (c_{p,k})$.

The elements of D_M are given by [30]

$$d_{p,k} = \begin{cases} \sqrt{\frac{2}{2k+1}} \frac{2^{\frac{3k-p}{2}}}{\left(\frac{p-k}{2}\right)! \prod_{j=1}^{(p-k)/2} (2k+2j+1)} \frac{p!k!}{(2k)!}, & p-k = even \\ 0, & p-k-odd \end{cases}. \tag{3.25}$$

The orthogonality property leads to the following inverse moment transform

$$f(x,y) = \sum_{i=0}^{\infty} \sum_{j=0}^{\infty} P_i(x) P_j(x) L_{ij}^{(f)}. \tag{3.26}$$

If only the moments of order up to (M, M) are computed, Eq.(3.26) is approximated by

$$f(x,y) \approx \sum_{i=0}^{M} \sum_{j=0}^{M} P_i(x) P_j(x) L_{ij}^{(f)}. \tag{3.27}$$

In the next, we will establish a relationship between the Legendre moments of an affine transformed image and those of the original image. The affine transformation can be represented by [26]

$$\begin{pmatrix} x' \\ y' \end{pmatrix} = A \begin{pmatrix} x \\ y \end{pmatrix} + \begin{pmatrix} x_0 \\ y_0 \end{pmatrix}, \tag{3.28}$$

where $A = \begin{pmatrix} a_{11} & a_{12} \\ a_{21} & a_{22} \end{pmatrix}$ is called the homogeneous affine transformation matrix.

The translation invariance can be achieved by locating the origin of the coordinate system to the center of mass of the object, that is, $L_{01}^{(f)} = L_{10}^{(f)} = 0$. Thus, (x_0, y_0) can be ignored and only the matrix A is taken into consideration in the following.

The 2D $(p+q)$-th order Legendre moment of the affine transformed image $f(x', y')$ is defined by

$$\begin{aligned} L_{p,q}^{(g)} &= \int_{-1}^{1}\int_{-1}^{1} P_p(x') P_q(y') f(x',y')\, dx'dy' \\ &= \det(A) \int_{-1}^{1}\int_{-1}^{1} P_p(a_{11}x + a_{12}y) P_q(a_{21}x + a_{22}y) f(x,y)\, dxdy, \end{aligned} \tag{3.29}$$

where $\det(A)$ denotes the determinant of the matrix A.

In the following, we discuss the way to express the Legendre moments of the affine transformed image defined by Eq.(3.29) in terms of Legendre moments of the original image.

By replacing the variable x by $a_{11}x + a_{12}y$ in Eq.(3.22), we have

$$\begin{aligned} P_p(a_{11}x + a_{12}y) &= \sum_{m=0}^{p} c_{p,m} (a_{11}x + a_{12}y)^m \\ &= \sum_{m=0}^{p}\sum_{s=0}^{m} \binom{m}{s} c_{p,m} a_{11}^s a_{12}^{m-s} x^s y^{m-s}. \end{aligned} \tag{3.30}$$

Similarly

$$P_q(a_{21}x + a_{22}y) = \sum_{n=0}^{p}\sum_{t=0}^{n} \binom{n}{t} c_{q,n} a_{21}^t a_{22}^{n-t} x^t y^{n-t}. \tag{3.31}$$

Substituting Eq.(3.30) and Eq.(3.31) into Eq.(3.29) yields

$$\begin{aligned} L_{p,q}^{(g)} = \det(A) \int_{-1}^{1}\int_{-1}^{1} \sum_{m=0}^{p}\sum_{s=0}^{m}\sum_{n=0}^{q}\sum_{t=0}^{n} \binom{m}{s}\binom{n}{t} \times \\ c_{p,m}c_{q,n} a_{11}^s a_{12}^{m-s} a_{21}^t a_{22}^{n-t} x^{s+t} y^{m+n-s-t} f(x,y)\, dxdy. \end{aligned} \tag{3.32}$$

Using Eq.(3.24), we have

$$x^{s+t} = \sum_{i=0}^{s+t} d_{s+t,i} P_i(x), \; y^{m+n-s-t} = \sum_{j=0}^{m+n-s-t} d_{m+n-s-t,j} P_j(y). \tag{3.33}$$

Substitution of Eq.(3.33) into Eq.(3.32) leads to

$$\begin{aligned} L_{p,q}^{(g)} = \det(A) \sum_{m=0}^{p}\sum_{n=0}^{q}\sum_{s=0}^{m}\sum_{t=0}^{n}\sum_{i=0}^{s+t}\sum_{j=0}^{m+n-s-t} \binom{m}{s}\binom{n}{t} \times \\ (a_{11})^s (a_{12})^{m-s} (a_{21})^t (a_{22})^{n-t} c_{p,m}c_{q,n} d_{s+t,i} d_{m+n-s-t,j} L_{ij}^{(f)}. \end{aligned} \tag{3.34}$$

Equation 3.34 shows that the Legendre moments of the transformed image can be expressed as a linear combination of those of the original image.

The direct use of Eq.(3.34) leads to a complex non-linear systems of equations. To avoid this, the homogeneous affine transformation matrix A is usually decomposed into a product of simple matrices. The decompositions mentioned above, known as XSR and XYS decompositions [26, 41], can be used.

The XSR decomposition decomposes the affine matrix A into an x-shearing, an anisotropic scaling and a rotation matrix as follows

$$\begin{bmatrix} a_{11} & a_{12} \\ a_{21} & a_{22} \end{bmatrix} = \begin{bmatrix} \cos\theta & \sin\theta \\ -\sin\theta & \cos\theta \end{bmatrix} \begin{bmatrix} \lambda & 0 \\ 0 & \mu \end{bmatrix} \begin{bmatrix} 1 & \rho \\ 0 & 1 \end{bmatrix}, \tag{3.35}$$

where λ, μ and ρ are real numbers, and θ is the rotation angle between 0 and 2π.

The XYS decomposition relies on decomposing the affine matrix A into an x-shearing, an y-shearing and an anisotropic scaling matrix, that is

$$\begin{bmatrix} a_{11} & a_{12} \\ a_{21} & a_{22} \end{bmatrix} = \begin{bmatrix} a & 0 \\ 0 & \delta \end{bmatrix} \begin{bmatrix} 1 & 0 \\ \gamma & 1 \end{bmatrix} \begin{bmatrix} 1 & \beta \\ 0 & 1 \end{bmatrix}, \tag{3.36}$$

where a, β , δ and γ are real numbers.

We adopt here the XYS decomposition. The same reasoning can be applied to the XSR decomposition. Using Eq.(3.34), we can derive a set of affine Legendre moment invariants (ALMIs) based on the following theorems.

Theorem 2. *For given integers p and q, let*

$$I_{pq}^{xsh} = \sum_{m=0}^{p}\sum_{n=0}^{q}\sum_{s=0}^{m}\sum_{i=0}^{s}\sum_{j=0}^{m+n-s} \binom{m}{s} \beta^{m-s} c_{p,m} c_{q,n} d_{s,i} d_{m+n-s,j} L_{ij}, \tag{3.37}$$

then I_{pq}^{xsh} are invariant to x-shearing.

The proof of Theorem 2 is available in [37].

Theorem 3. Let

$$I_{pq}^{ysh} = \sum_{m=0}^{p}\sum_{n=0}^{q}\sum_{t=0}^{n}\sum_{i=0}^{m+t}\sum_{j=0}^{n-t} \binom{n}{t} \gamma^{t} c_{p,m} c_{q,n} d_{m+t,i} d_{n-t,j} L_{ij}, \tag{3.38}$$

then I_{pq}^{ysh} are invariant to y-shearing.

The proof of Theorem 3 is very similar to that of Theorem 2 as pointed out in [37].

Theorem 4. *Let*

$$I_{pq}^{\alpha s} = \sum_{m=0}^{p}\sum_{n=0}^{q}\sum_{i=0}^{m}\sum_{j=0}^{n} \alpha^{m+1} \delta^{n+1} c_{p,m} c_{q,n} d_{m,i} d_{n,j} L_{ij}, \tag{3.39}$$

then $I_{pq}^{\alpha s}$ are invariant to anisotropic scaling.

Refer also to [37] for the proof of Theorem 4. Notice that we can easily derive the following theorem.

Theorem 5. *The Legendre moments of an image can be expressed as a linear combination of their invariants as follows:*

$$L_{pq} = \sum_{m=0}^{p}\sum_{n=0}^{q}\sum_{s=0}^{m}\sum_{i=0}^{s}\sum_{j=0}^{m+n-s}\binom{m}{s}(-\beta)^{m-s}c_{p,m}c_{q,n}d_{s,i}d_{m+n-s,j}I_{ij}^{xsh}, \tag{3.40}$$

$$L_{pq} = \sum_{m=0}^{p}\sum_{n=0}^{q}\sum_{t=0}^{n}\sum_{i=0}^{m+t}\sum_{j=0}^{n-t}\binom{n}{t}(-\gamma)^{t}c_{p,m}c_{q,n}d_{m+t,i}d_{n-t,j}I_{ij}^{ysh}, \tag{3.41}$$

$$L_{pq} = \sum_{m=0}^{p}\sum_{n=0}^{q}\sum_{i=0}^{m}\sum_{j=0}^{n}\alpha^{-(m+1)}\delta^{-(n+1)}c_{p,m}c_{q,n}d_{m,i}d_{n,j}I_{ij}^{\alpha s}. \tag{3.42}$$

The above equations show that the set of invariants is complete.

From this standpoint, by combining I_{pq}^{xsh}, I_{pq}^{ysh}, $I_{pq}^{\alpha s}$, that are respectively invariant to x-shearing, y-shearing and anisotropic scaling, we can obtain a set of ALMIs. For an image $f(x,y)$, we use the following process:

Step 1: x-shearing Legendre moment invariants are calculated by Eq.(3.37), where the Legendre moments L_{ij} are computed with Eq.(3.21).
Step 2: The combined invariants with respect to x-shearing and y-shearing are calculated by Eq.(3.38) where the Legendre moments on the right-hand side of Eq.(3.38) are replaced by computed in Step 1.
Step 3: The affine Legendre moment invariants are calculated by Eq.(3.39) where the Legendre moments on the right-hand side of Eq.(3.39) are replaced by computed in Step 2.

Because the parameters β_f, γ_f, α_f and δ_f in Eqs.(3.37)-(3.39) are image dependent, they must be estimated. Considering an affine transform and its XYS decomposition, by setting $I_{30}^{xsh}=0$ in Eq.(3.37), we have

$$L_{03}\beta^3+\frac{\sqrt{105}}{3}L_{12}\beta^2+\frac{\sqrt{105}}{3}L_{21}\beta+L_{30}=0. \tag{3.43}$$

The parameter β can then be determined by solving Eq.(3.43).

From Eq.(3.38), we have

$$I_{11}^{ysh}=\gamma\left(L_{00}+\frac{2}{\sqrt{5}}L_{20}\right)+L_{11}. \tag{3.44}$$

Letting $I_{11}^{ysh}=0$, we obtain

$$\gamma=-\frac{L_{11}}{L_{00}+\frac{2}{\sqrt{5}}L_{20}}. \tag{3.45}$$

Setting $I_{20}^{as} = I_{02}^{as} = 1$, we have

$$\alpha = \frac{\sqrt{b^2 + 4a} - b}{2a}, \quad \delta = \frac{\sqrt{b'^2 + 4a'} - b'}{2a'}, \tag{3.46}$$

where

$$\begin{gathered} a = \sqrt{\frac{V^3}{U}}, \; b = -\frac{\sqrt{5}}{2} L_{00} \sqrt{\frac{V}{U}}, \; a' = \sqrt{\frac{U^3}{V}}, \; b' = -\frac{\sqrt{5}}{2} L_{00} \sqrt{\frac{U}{V}}, \\ U = L_{02} + \frac{\sqrt{5}}{2} L_{00}, \; V = L_{20} + \frac{\sqrt{5}}{2} L_{00}. \end{gathered} \tag{3.47}$$

The parameters β_g, γ_g, α_g and δ_g associated with the transformed image $g(x, y)$ can also be estimated according to Eqs.(3.43), (3.45) and (3.46). It can be verified that the parameters provided by the above method satisfy the following relationships: $\beta_f = \beta_g + \beta_0$, $\gamma_f = \gamma_g + \gamma_0$, $\alpha_f = \alpha_0 \alpha_g$ and $\delta_f = \delta_0 \delta_g$, where α_0, β_0, γ_0 and δ_0 are the coefficients of the affine transform applied to f. Based on these relationships, the conditions given in Theorems 2 to 4 are satisfied. It is worth noting that other choice of parameters can also be made to keep the invariance of Eqs.(3.37)-(3.39) to image transformation.

To illustrate this section, a result extracted from a watermarking application has been selected [37]. Image watermarking aimed at responding to copyright protection concerns. To be efficient, such watermarking must be robust against a variety of attacks among which geometric distortions. In [37], affine invariants derived from Legendre moments were used. Watermark embedding and detection were directly performed on this set of invariants. Moreover, these moments were exploited for estimating the geometric distortion parameters in order to permit watermark extraction. Figure 3.2.2a shows the watermark used. It was embedded in four standard images further attacked by affine transformations (Fig.(3.2.2b) to (3.2.2e)). The size of the watermark image in that case is equal to the initial sizes of embedding images. The extracted watermarks in these respective images are depicted in Fig.(3.2.2f) to (3.2.2i) and it can easily be seen that they are correctly recovered even if a certain loss in quality is observed.

3.3 Derivation of Moment Invariants to Blur, and Combined Invariants to Geometric Transformation and to Blur

Because the real sensing systems are usually imperfect and the environmental conditions are changing over time, the acquired images often provide a degraded version of the true scene. An important class of degradations we are faced with in practice is image blurring, which can be caused by diffraction, lens aberration, wrong focus, and atmospheric turbulence. Blurring can be usually described by a convolution of an unknown original image with a space invariant point spread function (PSF). In pattern recognition, for instance, two options have been widely explored either through a two-step approach by restoring the image and then applying recognition methods, or by designing a direct one-step solution, free of blurring effects. In the former case, the

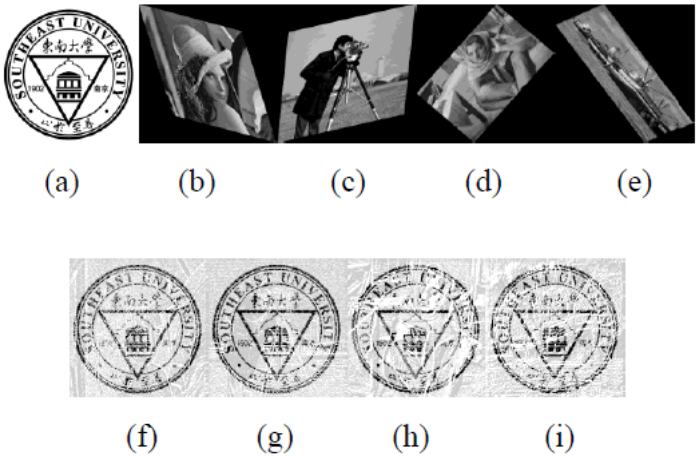

Figure 3.2: (a) Logo used as watermark. (b)-(e) Watermarked images under affine transformation. (f)-(i) Extracted watermark from (b)-(e). With permission.

point spread function, most often unknown in real applications, should be estimated. In the latter case, finding a set of invariants that are not affected by blurring is the key problem.

The pioneering work in this field was performed by Flusser et al. [10] who derived invariants to convolution with an arbitrary centrosymmetric PSF. These invariants have been successfully used in template matching of satellite images, in pattern recognition, in blurred digit and character recognition, in normalizing blurred images into canonical forms, and in focus/defocus quantitative measurement. More recently, Flusser and Zitova introduced the combined blur-rotation invariants [12] and reported their successful application to satellite image registration and camera motion estimation. Suk and Flusser further proposed a set of combined invariants which are invariant to affine transform and to blur [31]. The extension of blur invariants to N-dimensions has also been investigated [8, 1]. All the existing methods to derive the blur invariants are based on geometric moments or complex moments. However, both geometric moments and complex moments contain redundant information and are sensitive to noise especially when high-order moments are concerned. This is due to the fact that the kernel polynomials are not orthogonal. Since the orthogonal moments are better than other types of moments in terms of information redundancy, and are more robust to noise, it could be expected that the use of orthogonal moments in the construction of blur invariant provides better recognition results.

The second part of this chapter is aimed at showing how to construct a set of blur invariants by means of orthogonal moments.

3.3.1 Derivation of Invariants to Blur by Legendre Moments

We first review the theory of blur invariants of geometric moments reported in [30, 37], and then we present some basic definitions of Legendre moments.

A. Blur Invariants of Geometric Moments

The 2D geometric central moment of order $(p+q)$, with image intensity function $f(x,y)$, is defined as

$$\mu_{pq}^{(f)} = \int_{-1}^{1}\int_{-1}^{1} \left(x - x_c^{(f)}\right)^p \left(y - y_c^{(f)}\right)^q f(x,y)\, dxdy, \tag{3.48}$$

where, without loss of generality, we assume that the image function $f(x,y)$ is defined on the square $[-1,1]\times[-1,1]$. $\left(x_c^{(f)}, y_c^{(f)}\right)$ denotes the centroid of $f(x,y)$, which is defined by Eq.(3.6).

Let $g(x,y)$ be a blurred version of the original image $f(x,y)$. The blurring is classically described by the convolution

$$g(x,y) = (f * h)(x,y), \tag{3.49}$$

where $h(x,y)$ is the PSF of the imaging system, and $*$ denotes the linear convolution.

Assuming that the PSF, $h(x,y)$, is a centrally symmetric image function and the imaging system is energy-preserving, that is

$$h(x,y) = h(-x,-y), \tag{3.50}$$

$$\int_{-1}^{1}\int_{-1}^{1} h(x,y)\, dxdy = 1. \tag{3.51}$$

As noted by Flusser et al. [10], the assumption of centrally symmetry is not a significant limitation of practical utilization of the method. Most real sensors and imaging systems have PSFs with certain degrees of symmetry. In many cases they have even higher symmetry than central, such as axial or radial symmetry. Thus, the central symmetry assumption is general enough to describe almost all practical situations.

Lemma 1 [10]. *The centroid of the blurred image $g(x,y)$ is related to the centroid of the original image $f(x,y)$ and that of the PSF $h(x,y)$ as*

$$\begin{aligned} x_c^{(g)} &= x_c^{(f)} + x_c^{(h)}, \\ y_c^{(g)} &= y_c^{(f)} + y_c^{(h)}, \end{aligned} \tag{3.52}$$

In particular, if $h(x,y)$ is centrally symmetric, then $x_c^{(h)} = y_c^{(h)} = 0$. In such a case, we have $x_c^{(g)} = x_c^{(f)}$, $y_c^{(g)} = y_c^{(f)}$.

B. Blur Invariants of Legendre Moments

The 2D $(p+q)$-th order Legendre central moment of image intensity function $f(x,y)$, is defined as

$$\overline{L}_{pq}^{(f)} = \int_{-1}^{1}\int_{-1}^{1} P_p\left(x - x_c^{(f)}\right) P_q\left(y - y_c^{(f)}\right) f(x,y)\,dxdy,\ p,q = 0,1,2,..., \quad (3.53)$$

where $P_p(x)$ is the p-th order orthonormal Legendre polynomials given by Eq.(3.22).

In the following, we first establish a relationship between the Legendre moments of the blurred image and those of the original image and the PSF. We then derive a set of blur moment invariants.

The 2D normalized Legendre moments of a blurred image, $g(x,y)$, are defined by

$$\begin{aligned} L_{p,q}^{(g)} &= \int_{-1}^{1}\int_{-1}^{1} P_p(x) P_q(y) g(x,y)\,dxdy \\ &= \int_{-1}^{1}\int_{-1}^{1} P_p(x) P_q(y) (f * h)(x,y)\,dxdy \\ &= \int_{-1}^{1}\int_{-1}^{1} P_p(x) P_q(y) \left(\int_{-\infty}^{\infty}\int_{-\infty}^{\infty} h(a,b) f(x-a,y-b)\,dadb\right) dxdy \\ &= \int_{-1}^{1}\int_{-1}^{1} h(a,b) \left(\int_{-1}^{1}\int_{-1}^{1} P_p(x+a) P_q(y+b) f(x,y)\,dxdy\right) dadb. \end{aligned} \quad (3.54)$$

The following theorem reveals the relationship between the Legendre moments of the blurred image and those of the original image and the PSF.

Theorem 6. *Let $f(x,y)$ be the original image function and the PSF $h(x,y)$ be an arbitrary image function, and $g(x,y)$ be a blurred version of $f(x,y)$, then the relations*

$$L_{p,q}^{(g)} = \sum_{i=0}^{p}\sum_{j=0}^{q} L_{i,j}^{(f)} \sum_{s=0}^{p-i}\sum_{t=0}^{q-j} L_{s,t}^{(h)} \sum_{k=i}^{p-s}\sum_{m=k+s}^{p}\sum_{l=j}^{q-t}\sum_{n=l+t}^{q} \binom{m}{k}\binom{n}{l} \times c_{p,m} c_{q,n} d_{k,i} d_{m-k,s} d_{l,j} d_{n-l,t} \quad (3.55)$$

and

$$\overline{L}_{p,q}^{(g)} = \sum_{i=0}^{p}\sum_{j=0}^{q} \overline{L}_{i,j}^{(f)} \sum_{s=0}^{p-i}\sum_{t=0}^{q-j} \overline{L}_{s,t}^{(h)} \sum_{k=i}^{p-s}\sum_{m=k+s}^{p}\sum_{l=j}^{q-t}\sum_{n=l+t}^{q} \binom{m}{k}\binom{n}{l} \times c_{p,m} c_{q,n} d_{k,i} d_{m-k,s} d_{l,j} d_{n-l,t}. \quad (3.56)$$

hold for every p and q.
We further have the following result.

Theorem 7. *If $h(x,y)$ satisfies the conditions of central symmetry, then*

(a) $L_{p,q}^{(h)} = \overline{L}_{p,q}^{(h)}$ for every p and q;

(b) $L_{p,q}^{(h)} = 0$ if $(p+q)$ is odd.

The proof of the above two theorems can be found in [38].

With the help of Theorems 6 and 7, we are now ready to construct a set of blur invariants of Legendre moments through the following theorem.

Theorem 8. *Let $f(x,y)$ be an image function. Let us define the following function $I^{(f)} : N \times N \longrightarrow \mathbb{R}$.*

If $(p+q)$ is even then

$$I(p,q)^{(f)} = 0.$$

if $(p+q)$ is odd then

$$\begin{aligned} I(p,q)^{(f)} =& L_{p,q}^{(f)} - \frac{1}{2L_{0,0}^{(f)}} \sum_{i=0}^{p} \sum_{\substack{j=0 \\ 0<i+j<p+q}}^{q} I(i,j)^{(f)} \sum_{s=0}^{p-i} \sum_{t=0}^{q-j} L_{s,t}^{(f)} \\ & \sum_{k=i}^{p-s} \sum_{m=k+s}^{p} \sum_{l=j}^{q-t} \sum_{n=l+t}^{q} \begin{pmatrix} m \\ k \end{pmatrix} \times \begin{pmatrix} n \\ l \end{pmatrix} c_{p,m} c_{q,n} d_{k,i} d_{m-k,s} d_{l,j} d_{n-l,t}. \end{aligned} \tag{3.57}$$

Therefore, $I(p,q)$ is invariant to centrally symmetric blur for any p and q. The number $(p+q)$ is called the order of the invariant. The proof of Theorem 8 is also given in [38].

Using the Legendre central moments instead of Legendre moments, we can obtain a set of invariants to translation and to blur which are formally similar to $I(p,q)^{(f)}$.

Theorem 9. *Let $f(x,y)$ be an image function. Let us define the following function $\overline{I}^{(f)} : N \times N \longrightarrow \mathbb{R}$.*

If $(p+q)$ is even then

$$\overline{I}(p,q)^{(f)} = 0.$$

if $(p+q)$ is odd then

Figure 3.3: Eight objects selected from the Coil-100 image database of Columbia University. With permission.

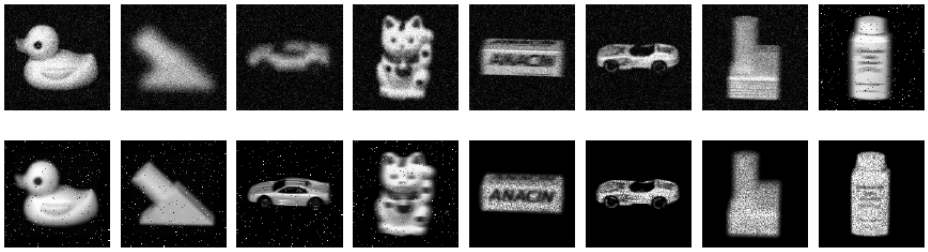

Figure 3.4: Some examples of the blurred images corrupted by various types of noise. With permission.

$$\overline{I}\,(p,q)^{(f)} = L_{p,q}^{(f)} - \frac{1}{2\overline{L}_{0,0}^{(f)}} \sum_{i=0}^{p} \sum_{\substack{j=0 \\ 0<i+j<p+q}}^{q} \overline{I}\,(i,j)^{(f)} \sum_{s=0}^{p-i} \sum_{t=0}^{q-j} \overline{L}_{s,t}^{(f)} \sum_{k=i}^{p-s} \sum_{m=k+s}^{p} \sum_{l=j}^{q-t} \sum_{n=l+t}^{q} \begin{pmatrix} m \\ k \end{pmatrix} \times \begin{pmatrix} n \\ l \end{pmatrix} c_{p,m} c_{q,n} d_{k,i} d_{m-k,s} d_{l,j} d_{n-l,t}. \tag{3.58}$$

Thus $\overline{I}\,(p,q)^{(f)}$, is invariant to centrally symmetric blur and to translation for any p and q.

It should be noted that $\overline{I}\,(p,q)$ in Eq.(3.58) deals with translation of both the image and the PSF. Based on Eq.(3.58), we can construct a set of blur and translation invariants of Legendre moments and express them in explicit form. The invariants of the third, fifth and seventh orders are listed in Appendix.

Partial results of the method reported in [38] for blurred image recognition by Legendre moment invariants will serve as an example of what can be expected in terms of performance. The original images were selected from the Coil-100 image database of Columbia University (size 160×160), which are shown in Fig.(3.3). They were blurred by means of averaging blur, out-of-focus blur, Gaussian blur and motion blur with different mask sizes and corrupted by additive Gaussian noise or salt-and-pepper noise (see Fig.(3.4) for some samples). Table 3.1 provides a comparison between geometric moments invariants (GMI), complex moment invariants (CMI) and Legendre moment invariants (LMI). Only the highest levels of noise are considered here.

This table shows that all moments behave well in noise-free situations. Relatively poor classification rates are observed when the noise level is high. LMIs perfom better

Table 3.1: The recognition rates of the GMI, CMI and LMI in object recognition (Fig.4). With permission.

	GMI	CMI	LMI
Noise-free	100%	100%	100%
Additive white noise with STD=8	78.33%	80%	96.25%
Additive white noise with STD=25	60.42%	50.62%	74.79%
Additive salt-and-pepper noise with noise density = 0.03	68.13%	56.46%	79.37%
Additive multiplicative noise with noise density = 0.5	90%	81.88%	95.63%
Computation time	9.42s	44.14s	9.80s

than GMIs and CMIs. The classification rates are higher than 95% but show insufficient performance in some cases. The computational times are also indicated. The implementations were done in MATLAB 6.5 on a PC P4 2.4 GHZ, 512 M RAM. More detailed experimentations and results can be found in [38].

3.3.2 Combined Invariants to Similarity and to Blur by Zernike Moments

We have proposed in the previous section an approach based on the orthogonal Legendre moments to derive a set of blur invariants. It has been shown in [38] that they are more robust to noise and have better discriminative power than the existing methods. However, one weak point of Legendre moment descriptors is that they are only invariant to translation, but not invariant under image rotation and scaling. Zhu et al. [42] and Ji and Zhu [15] proposed the use of the Zernike moments to construct a set of combined blur-rotation invariants. Unfortunately, there are two limitations to their methods: (1) only a Gaussian blur has been taken into account, which is a special case of PSF having circularly symmetry; (2) only a subset of Zernike moments of order p with repetition p, $Z_{p,p}$, has been used in the derivation of invariants. Since $Z_{p,p}$ corresponds to the radial moment $D_{p,p}$ or the complex moment $C_{0,p}$ if neglecting the normalization factor, the set of invariants constructed by Zhu et al. is a subset of that proposed by Flusser [13].

Here, we propose a new method to derive a set of combined geometric-blur invariants based on orthogonal Zernike moments. We further assume that the applied PSF is circularly symmetric. The reasons for such a choice of PSF are as follows [13]: (1) the majority of the PSFs occurring in real situations exhibit a circular symmetry; (2) since the PSFs having circular symmetry are a subset of centrosymmetric functions, it could be expected that we can derive some new invariants. In fact, the previously reported convolution invariants with centrosymmetric PSF include only the odd order moments. Flusser and Zitova [13] have shown that there exist even order moment invariants with circularly symmetric PSF. The radial moment of order p with repetition q of image intensity function $f(r,\theta)$ is defined as

$$D_{p,q}^{(f)} = \int_0^{2\pi}\int_0^1 r^p e^{-\hat{j}q\theta} f(r,\theta)\, r dr d\theta, \tag{3.59}$$

with $\hat{j} = \sqrt{-1}$, $0 \le r \le 1$, $p \ge 0$, $q = 0, \pm 1, \pm 2, ...$The Zernike moment of order p with repetition q of $f(r,\theta)$ is defined as [35]

$$Z_{p,q}^{(f)} = \frac{p+1}{\pi}\int_0^{2\pi}\int_0^1 R_{p,q}(r)\, e^{-\hat{j}q\theta} f(r,\theta)\, r dr d\theta,\ p \ge 0,\ |q| \le p,\ p-|q|\, being\, even, \tag{3.60}$$

where $R_{p,q}(r)$is the real-valued radial polynomial given by

$$R_{p,q}(r) = \sum_{k=0}^{(p-|q|)/2} \frac{(-1)^k (p-k)!}{k!\left(\frac{p+|q|}{2}-k\right)!\left(\frac{p-|q|}{2}-k\right)!} r^{p-2k}. \tag{3.61}$$

The above equation shows that the radial polynomial $R_{p,q}(r)$ is symmetric with q, that is, $R_{p,-q}(r) = R_{p,q}(r)$, for $q \ge 0$. Thus, we can consider the case where $q \ge 0$. Letting $p = q + 2l$ in Eq.(3.61) with $l \ge 0$, and substituting it into Eq.(3.60) yields

$$\begin{aligned}
Z_{q+2l,q}^{(f)} &= \frac{q+2l+1}{\pi}\int_0^{2\pi}\int_0^1 \left[\sum_{k=0}^{l}(-1)^k \frac{(q+2l-k)!}{k!\,(q+l-k)!\,(l-k)!} r^{q+2(l-k)}\right]\times \\
&\quad e^{-\hat{j}q\theta} f(r,\theta)\, r dr d\theta \\
&= \frac{q+2l+1}{\pi}\int_0^{2\pi}\int_0^1 \left[\sum_{k=0}^{l}(-1)^{l-k} \frac{(q+l+k)!}{k!\,(q+k)!\,(l-k)!} r^{q+2k}\right]\times \\
&\quad e^{-\hat{j}q\theta} f(r,\theta)\, r dr d\theta \\
&= \sum_{k=0}^{l}(-1)^{l-k}\frac{q+2l+1}{\pi}\frac{(q+l+k)!}{k!\,(q+k)!\,(l-k)!}\int_0^{2\pi}\int_0^1 r^{q+2k}\times \\
&\quad e^{-\hat{j}q\theta} f(r,\theta)\, r dr d\theta \\
&= \sum_{k=0}^{l} c_{l,k}^{q} D_{q+2k,q}^{(f)},
\end{aligned} \tag{3.62}$$

where

$$c_{l,k}^{q} = (-1)^{l-k}\frac{q+2l+1}{\pi}\frac{(q+l+k)!}{k!\,(q+k)!\,(l-k)!} \tag{3.63}$$

Let f' be a rotated version of f, i. e. $f'(r,\theta) = f(r,\theta-\beta)$, where β is the angle of rotation, and let $Z_{q+2l,q}^{(f')}$be the Zernike moments of f' . It can be seen from Eq.(3.61) that

$$Z_{q+2l,q}^{(f')} = e^{-\hat{j}q\beta} Z_{q+2l,q}^{(f)}. \tag{3.64}$$

Let $g(x,y)$ be a blurred version of the original image , and $h(x,y)$ be the PSF of the imaging system. We assume that the PSF, $h(x,y)$, is a circularly symmetric image function, and that the imaging system is energy-preserving, which leads to

$$h(x,y) = h(r,\theta) = h(r), \tag{3.65}$$

$$\int\int h(x,y)\,dxdy = 1. \tag{3.66}$$

Under the assumption of Eq.(3.65), the Zernike moments of$h(r,\theta)$ equal those of any rotated image h'. Combining this fact with Eq.(3.64), we get

$$Z_{q+2l,q}^{(h)} = Z_{q+2l,q}^{(h')} = e^{-\hat{j}q\beta} Z_{q+2l,q}^{(h)}. \tag{3.67}$$

Equation 3.67 is verified if and only if either $Z_{q+2l,q}^{(h)} = 0$ or $q = 0$. Thus, an important property of circularly symmetric functions can be stated as follows.

Proposition 2. *If $q \neq 0$ and $h(r,\theta)$ is a circularly symmetric image function, then* $Z_{q+2l,q}^{(h)} = 0$ for any non-negative integer l.

The proof of Proposition 2 can be found in [2].

We can now establish the relationship between the Zernike moments of the blurred image and those of the original image and the PSF. To that end, we first consider the radial moments. Applying Eq.(3.59) to blurred image $g(x,y)$, we have

$$\begin{aligned} D_{q+2k,q}^{(g)} &= \int_{-\infty}^{\infty}\int_{-\infty}^{\infty} \left(x-\hat{j}y\right)^{q+k} \left(x+\hat{j}y\right)^{k} g(x,y)\,dxdy \\ &= \int_{-\infty}^{\infty}\int_{-\infty}^{\infty} \left(x-\hat{j}y\right)^{q+k} \left(x+\hat{j}y\right)^{k} \times \\ &\quad \left[\int_{-\infty}^{\infty}\int_{-\infty}^{\infty} h(a,b)\,f(x-a,y-b)\,dadb\right] dxdy \\ &= \int_{-\infty}^{\infty}\int_{-\infty}^{\infty} h(a,b)\,T(a,b)\,dadb \end{aligned} \tag{3.68}$$

with

$$\begin{aligned} T(a,b) = \int_{-\infty}^{\infty}\int_{-\infty}^{\infty} &\left(\left(x-\hat{j}y\right)+\left(a-\hat{j}b\right)\right)^{q+k} \times \\ &\left(\left(x+\hat{j}y\right)+\left(a+\hat{j}b\right)\right)^{k} f(x,y)\,dxdy. \end{aligned}$$

Finally, Eq.(3.68) take the form

$$D^{(g)}_{q+2k,q} = \sum_{m=0}^{q+k}\sum_{n=0}^{k}\left(\begin{array}{c} q+k \\ m \end{array}\right)\left(\begin{array}{c} k \\ n \end{array}\right) D^{(f)}_{m+n,m-n} D^{(h)}_{q+2k-m-n,q+n-m}. \tag{3.69}$$

Applying Eq.(3.62) to blurred image $g(x,y) = g(r,\theta)$ and using Eq.(3.69), we obtain

$$Z^{(g)}_{q+2l,q} = \sum_{k=0}^{l}\sum_{m=0}^{q+k}\sum_{n=0}^{k}\left(\begin{array}{c} q+k \\ m \end{array}\right)\left(\begin{array}{c} k \\ n \end{array}\right) c^{q}_{l,k} D^{(f)}_{m+n,m-n} D^{(h)}_{q+2k-m-n,q+n-m}. \tag{3.70}$$

From Eq.(3.62), the radial moments can also be expressed as a series of Zernike moments

$$D^{(f)}_{q+2l.q} = \sum_{k=0}^{l} d^{q}_{l,k} Z^{(f)}_{q+2k,q}, \tag{3.71}$$

where $D^{q}_{l} = \left(d^{q}_{i,j}\right), 0 \le j \le i \le l$, is the inverse matrix of $C^{q}_{l} = \left(c^{q}_{i,j}\right)$. Both C^{q}_{l} and D^{q}_{l} are lower triangular matrices of size $(l+1)\times(l+1)$, the elements of C^{q}_{l} are given by Eq.(3.63). The elements of D^{q}_{l} are given by [29]

$$d^{q}_{i,j} = \frac{i!\,(q+i)!\pi}{(i-j)!\,(q+i+j+1)!},\ 0 \le j \le i \le l. \tag{3.72}$$

From Eq.(3.71), we have

$$D^{(f)}_{m+n,m-n} = \sum_{i=0}^{n} d^{m-n}_{n,i} Z^{(f)}_{m-n+2i,m-n}, \tag{3.73}$$

$$D^{(h)}_{q+2k-m-n,q+n-m} = \sum_{j=0}^{k-n} d^{q+n-m}_{k-n,j} Z^{(h)}_{q+n-m+2j,q+n-m}, \tag{3.74}$$

By introducing Eq.(3.73) and Eq.(3.74) into Eq.(3.70), we obtain

$$\begin{aligned} Z^{(g)}_{q+2l,q} = &\sum_{k=0}^{l}\sum_{m=0}^{q+k}\sum_{n=0}^{k}\sum_{i=0}^{n}\sum_{j=0}^{k-n}\left(\begin{array}{c} q+k \\ m \end{array}\right)\left(\begin{array}{c} k \\ n \end{array}\right)\times \\ &c^{q}_{l,k} d^{m-n}_{n,i} d^{q+n-m}_{k-n,j} Z^{(f)}_{m-n+2i,m-n} Z^{(h)}_{q+n-m+2j,q+n-m}. \end{aligned} \tag{3.75}$$

Based on Eq.(3.75), we have the following theorem.

Theorem 10. *Let $f(r,\theta)$ be the original image function and the PSF $h(r,\theta)$ be circularly symmetric, $g(r,\theta)$ be a blurred version of $f(r,\theta)$, then the following relation*

$$Z_{q+2l,q}^{(g)} = \sum_{i=0}^{l} Z_{q+2i,q}^{(f)} \sum_{j=0}^{l-i} Z_{2j,0}^{(h)} A\left(q,l,i,j\right), \tag{3.76}$$

stands for any $q \geq 0$ *and* $l \geq 0$*, where the coefficients* $A\left(q,l,i,j\right)$ *are given by*

$$A\left(q,l,i,j\right) = \sum_{k=i+j}^{l} \sum_{n=i}^{k-j} \left(\begin{array}{c} q+k \\ q+n \end{array} \right) \left(\begin{array}{c} k \\ n \end{array} \right) c_{l,k}^{q} d_{n,i}^{q} d_{k-n,j}^{0}. \tag{3.77}$$

Its proof can also be found in [2].

Based on Theorem 10, it becomes possible to construct a set of blur invariants of Zernike moments through the following theorem.

Theorem 11. *Let* $f\left(r,\theta\right)$ *be an image function. Let us define the following function* $I^{(f)} : N \times N \longrightarrow \mathbb{R}$.

$$I\left(q+2l,q\right)^{(f)} = Z_{q+2l,q}^{(f)} - \frac{1}{Z_{0,0}^{(f)}\pi} \sum_{i=0}^{l-1} I\left(q+2i,q\right)^{(f)} \sum_{j=0}^{l-i} Z_{2j,,0}^{(f)} A\left(q,l,i,j\right). \tag{3.78}$$

Then $I\left(q+2l,q\right)^{(f)}$ *is invariant to circularly symmetric blur for any* $q \geq 0$ *and* $l \geq 0$*. The number* $p = q + 2l$ *is called the order of the invariant.*

The proof of Theorem 11 has been reported in [2].

Some remarks deserve to be made.

Remark 1. *By using the symmetric property of* $R_{p,q}\left(r\right)$ *with* q*, it can be easily proven that* $I\left(|q|+2l,q\right)^{(f)}$ *for* $q < 0$ *is also invariant to convolution.*

Remark 2. *It can be deduced from Eq.(3.78) that* $I\left(2l,0\right)^{(f)} = \left(-1\right)^{l}\left(2l+1\right) Z_{0,0}^{(f)}$*. Thus, only* $I\left(0,0\right)^{(f)} = Z_{0,0}^{(f)}$ *will be used as invariant for the case* $q = 0$*.*

Remark 3. *If we use the Zernike central moments* $\overline{Z}_{q+2l,q}^{(f)}$ *instead of Zernike moments in Eq.(3.78), then we can obtain a set of invariants* $\overline{I}\left(q+2l,q\right)^{(f)}$ *that is invariant to both translation and to blur.*

Based on Theorem 11, we can construct a set of blur invariants of Zernike moments with arbitrary order and express them in explicit form. The invariants up to sixth order are listed in the Appendix.

Lemma 2. *Let* f' *be a rotated version of* f*, i.e.,* $f''\left(r,\theta\right) = f\left(r,\theta-\beta\right)$*, where* β *denotes the rotation angle, then the following relation holds for any* $q \geq 0$ *and* $l \geq 0$

$$I\left(q+2l,q\right)^{(f')} = e^{-\hat{j}q\beta} I\left(q+2l,q\right)^{(f)}. \tag{3.79}$$

Lemma 3. *Let $f(r,\theta)$ be an image function. It holds for any $q \geq 0$ and $l \geq 0$ that*

$$I(q+2l,-q)^{(f)} = I^*(q+2l,q)^{(f)}, \tag{3.80}$$

where the superscript $*$ denotes the complex conjugate.

The proof of the two lemmas can be found in [2].

In the following, we construct a set of combined geometric-blur invariants. As already stated, the translation invariance can be achieved by using the central Zernike moments. Equation 3.79 shows that the magnitude of $I(q+2l,q)^{(f)}$ is invariant to rotation. However, the magnitudes do not yield a complete set of the invariants. Herein, we provide a way to build up such a set. Let f'' and f be two images having the same content but distinct orientation β and scale λ, that is, $f''(r,\theta) = f(r/\lambda, \theta-\beta)$, the Zernike moment of the transformed image is given by

$$\begin{aligned} Z_{q+2l,q}^{(f'')} &= \frac{q+2l+1}{\pi} \int_0^{2\pi}\int_0^1 R_{q+2l,q}(r)\, e^{-\hat{j}q\theta} f(r/\lambda, \theta-\beta)\, r dr d\theta \\ &= e^{-\hat{j}q\beta} \frac{q+2l+1}{\pi} \lambda^2 \int_0^{2\pi}\int_0^1 R_{q+2l,q}(\lambda r)\, e^{-\hat{j}q\theta} f(r,\theta)\, r dr d\theta. \end{aligned} \tag{3.81}$$

Using Eq.(3.62) and Eq.(3.71) we have

$$\begin{aligned} Z_{q+2l,q}^{(f'')} &= e^{-\hat{j}q\beta} \sum_{k=0}^{l} \lambda^{q+2k+2} c_{l,k}^q D_{q+2k,q}^{(f)} \\ &= e^{-\hat{j}q\beta} \sum_{k=0}^{l}\sum_{m=0}^{k} \lambda^{q+2k+2} c_{l,k}^q d_{k,m}^q Z_{q+2m,q}^{(f)} \\ &= e^{-\hat{j}q\beta} \sum_{m=0}^{l}\sum_{k=m}^{l} \lambda^{q+2k+2} c_{l,k}^q d_{k,m}^q Z_{q+2m,q}^{(f)}. \end{aligned} \tag{3.82}$$

Therefore, we have the following theorem:

Theorem 12. *Let*

$$L_{q+2l,q}^{(f')} = e^{-\hat{j}q\theta_f} \sum_{m=0}^{l}\sum_{k=m}^{l} \Gamma_f^{-(q+2k+2)} c_{l,k}^q d_{k,m}^q Z_{q+2m,q}^{(f)} \tag{3.83}$$

with $\theta_f = \arg\left(Z_{1,1}^{(f)}\right)$ and $\Gamma_f = \sqrt{Z_{0,0}^{(f)}}$. Then $L_{q+2l,q}^{(f')}$ is invariant to both image rotation and scaling for any non-negative integers q and l.

(a) (b) (c) (d)

Figure 3.5: Images of the outdoor scene. (a) The original image, (b) The transformed and blurred image, (c) The matched templates using CMIs, (d) The matched templates using the proposed ZMIs With permission.

Remark 4. *Many other choices of θ_f and Γ_f are possible. In fact, they can be chosen in such a way that we $\Gamma_{f''} = \lambda\Gamma_f$, $\theta_{f''} = \theta_f - \beta$ where $f''(r,\theta) = f(r/\lambda, \theta - \beta)$ is the transformed image of f. However, it is preferable to use the lower order moments because they are less sensitive to noise than the higher order ones. If the central moments are used, θ_f can be chosen as $\theta_f = \arg\left(Z_{3,1}^f\right)$.*

Theorem 13. *For any $q \geq 0$ and $l \geq 0$, let*

$$SI(q+2l,q)^{(f)} = e^{-\hat{j}q\theta_f} \sum_{m=0}^{l} \sum_{k=m}^{l} \Gamma_f^{-(q+2k+2)} c_{l,k}^q d_{k,m}^q I(q+2m,q)^{(f)}, \quad (3.84)$$

where $I(q+2m,q)^{(f)}$ is defined in Eq.(3.78). Then $SI(q+2l,q)^{(f)}$ is both invariant to convolution and to image scaling and rotation.

The proofs of Theorems 12 and 13 are given in [2]. The combined invariants up to sixth order are listed in Appendix.

For illustration purpose of this section, we take one of the examples depicted in [2]. It relies on a set of combined geometric-blur invariants derived from Zernike moments and aims at localizing templates in a real outdoor scene displayed in Fig.(3.5).

The initial images were acquired by a standard digital camera submitted to a rotation and an out-of-focus blur. Nine templates were extracted in the reference image (numbered from 1 to 9 in the left image). They were then searched in the transformed and blurred image by using a template matching procedure. The results show that the ZMIs lead to find all templates when CMIs fail to only detect part of them.

3.4 Conclusion

Although orthogonal moments and their respective invariants have attracted much interest all over the world these last years with both impressive theoretical contributions

and multiple applications, it is expected that this trend will continue and will open new paths in computer vision at large. The complexity of situations to handle (dense scenes, non-geometric/unstructured objects, large deformations, occlusions, projective transformations, etc), the strong competition with other methodological approaches (differential invariants, multi-scale methods, shape-based algorithms, shape from texture, etc) will continuously challenge the moment-based techniques. If most of the papers recently published are comparing moment-based methods (Zernike to Legendre and the like), more comparisons with different frames are required in order to assess when and where they bring a real superiority. Criteria such that robustness (to noise, deformations, blur, and so on), accuracy in localization (i.e. critical in matching and registration), distinctiveness (for discrimination purpose) and others can be considered for that.

Let us recall that moment invariants do solve only partially the computer vision problems. They have to be integrated in the full image processing scheme (from image acquisition to image interpretation). Specific constraints (large data sets to deal with, real-time or almost real-time processing) must also be taken into consideration to address practical problems: accelerated algorithms deserve interest to reduce the computation load. Following [16], special attention should be paid to a proper implementation of moment-based algorithms to preserve their orthogonality properties.

Acknowledgements

The authors are indebted to their master and PhD students Hui Zhang, Beijing Chen, Guanyu Yang, Jiasong Wu, Yining Hu and Hongqing Zhu for their contributions in the development of moment-based methods and the experiments they conducted to assess their interest in various applications.

These works have been made possible with the support of numerous grants among which the National Basic Research Program of China under Grants 2011CB707904 and 2010CB732503, the National Natural Science Foundation of China under Grants 61073138, 61271312, 61201344, 81101104, 31100713 and 11301074, the Ministry of Education of China under Grants 20110092110023 and 20120092120036, the Key Laboratory of Computer Network and Information Integration (Southeast University), Ministry of Education, the Qing Lan project, the Natural Science Foundation of Jiangsu Province under Grants BK2012329 and BK2012743, and Jiangsu Province under Grant DZXX-031. They are also part of the collaboration established for years between the Chinese (LIST) and French (LTSI) laboratories through the joint international research center, CRIBs.

Appendix A

The expressions given below provide to the interested readers all the elements to replicate our method and to apply it to other examples.

A1. List of Legendre moment invariants up to the seventh order

Third Order

$$\overline{I}(3,0) = \overline{L}_{30}$$
$$\overline{I}(2,1) = \overline{L}_{21}$$
$$\overline{I}(1,2) = \overline{L}_{12}$$
$$\overline{I}(0,3) = \overline{L}_{03}$$

Fifth Order

$$\overline{I}(5,0) = \overline{L}_{50} - \frac{3\sqrt{77}}{2}\overline{L}_{30} - \frac{3\sqrt{385}\,\overline{L}_{20}\overline{L}_{30}}{5\overline{L}_{00}}$$

$$\overline{I}(4,1) = \overline{L}_{41} - \frac{7\sqrt{5}}{2}\overline{L}_{21} - \frac{1}{\overline{L}_{00}}\left(7\overline{L}_{21}\overline{L}_{20} + \sqrt{21}\,\overline{L}_{11}\overline{L}_{30}\right)$$

$$\overline{I}(3,2) = \overline{L}_{32} - \frac{5}{6}\sqrt{21}\,\overline{L}_{12} - \frac{\sqrt{5}}{2}\overline{L}_{30} - \frac{1}{\overline{L}_{00}}\times \left(\frac{\sqrt{105}}{3}\overline{L}_{20}\overline{L}_{12} + \frac{5\sqrt{21}}{3}\overline{L}_{11}\overline{L}_{21} + \overline{L}_{02}\overline{L}_{30}\right)$$

$$\overline{I}(2,3) = \overline{L}_{23} - \frac{5}{6}\sqrt{21}\,\overline{L}_{21} - \frac{\sqrt{5}}{2}\overline{L}_{03} - \frac{1}{\overline{L}_{00}}\times \left(\frac{\sqrt{105}}{3}\overline{L}_{02}\overline{L}_{21} + \frac{5\sqrt{21}}{3}\overline{L}_{11}\overline{L}_{12} + \overline{L}_{20}\overline{L}_{03}\right)$$

$$\overline{I}(1,4) = \overline{L}_{14} - \frac{7\sqrt{5}}{2}\overline{L}_{12} - \frac{1}{\overline{L}_{00}}\left(7\overline{L}_{12}\overline{L}_{02} + \sqrt{21}\,\overline{L}_{11}\overline{L}_{03}\right)$$

$$\overline{I}(0,5) = \overline{L}_{05} - \frac{3\sqrt{77}}{2}\overline{L}_{03} - \frac{3\sqrt{385}\,\overline{L}_{02}\overline{L}_{03}}{5\overline{L}_{00}}$$

Seventh Order

$$\overline{I}(7,0) = \overline{L}_{70} - \frac{1727\sqrt{105}}{120}\overline{L}_{30} - \frac{13\sqrt{165}}{6}\overline{I}(5,0) - \frac{1}{\overline{L}_{00}}\left(\frac{1595\sqrt{21}}{42}\overline{L}_{20}\overline{L}_{30} + \frac{143\sqrt{105}}{35}\overline{L}_{40}\overline{L}_{30} + \frac{13\sqrt{33}}{3}\overline{L}_{20}\overline{I}(5,0)\right)$$

$$\begin{aligned}\overline{I}(6,1) =&\overline{L}_{61} - \frac{351\sqrt{65}}{40}\overline{L}_{21} - \frac{11\sqrt{13}}{2}\overline{I}(4,1) - \frac{1}{\overline{L}_{00}}\Bigg(\frac{45\sqrt{13}}{2}\overline{L}_{20}\overline{L}_{21}\\ &+ \frac{11\sqrt{65}}{5}\overline{L}_{40}\overline{L}_{21} + \frac{109\sqrt{273}}{30}\overline{L}_{11}\overline{L}_{30} + \frac{33\sqrt{13}}{5}\overline{L}_{31}\overline{L}_{30}\\ &+ \frac{11\sqrt{65}}{5}\overline{L}_{20}\overline{I}(4,1) + \frac{\sqrt{429}}{3}\overline{L}_{11}\overline{I}(5,0)\Bigg)\end{aligned}$$

$$\begin{aligned}\overline{I}(5,2) =&\overline{L}_{52} - \frac{119\sqrt{33}}{24}\overline{L}_{12} - \frac{3\sqrt{385}}{4}\overline{L}_{30} - \frac{3\sqrt{77}}{2}\overline{I}(3,2) - \frac{\sqrt{5}}{2}\overline{I}(5,0)\\ &- \frac{1}{\overline{L}_{00}}\Bigg(\frac{73\sqrt{165}}{30}\overline{L}_{20}\overline{L}_{12} + \sqrt{33}\,\overline{L}_{40}\overline{L}_{12} + \frac{73\sqrt{33}}{6}\overline{L}_{11}\overline{L}_{21}\\ &+ 3\sqrt{77}\,\overline{L}_{31}\overline{L}_{21} + \frac{3\sqrt{77}}{2}\overline{L}_{02}\overline{L}_{30} + \frac{3\sqrt{77}}{2}\overline{L}_{20}\overline{L}_{30}\\ &+ \frac{3\sqrt{385}}{5}\overline{L}_{22}\overline{L}_{30} + \frac{3\sqrt{385}}{5}\overline{L}_{20}\overline{I}(3,2)\sqrt{165}\,\overline{L}_{11}\overline{I}(4,1) + \overline{L}_{02}\overline{I}(5,0)\Bigg)\end{aligned}$$

$$\begin{aligned}\overline{I}(4,3) =&\overline{L}_{43} - \frac{61}{8}\overline{L}_{03} - \frac{35\sqrt{105}}{12}\overline{L}_{21} - \frac{7\sqrt{5}}{2}\overline{I}(2,3) - \frac{5\sqrt{21}}{6}\overline{I}(4,1)\\ &- \frac{1}{\overline{L}_{00}}\Bigg(\frac{7\sqrt{5}}{2}\overline{L}_{20}\overline{L}_{03} + \overline{L}_{40}\overline{L}_{03} + \frac{9\sqrt{105}}{2}\overline{L}_{11}\overline{L}_{12} + 7\sqrt{5}\,\overline{L}_{31}\overline{L}_{12}\\ &+ \frac{35\sqrt{21}}{6}\overline{L}_{02}\overline{L}_{21} + \frac{35\sqrt{21}}{6}\overline{L}_{20}\overline{L}_{21} + \frac{7\sqrt{105}}{3}\overline{L}_{22}\overline{L}_{21} + 7\overline{L}_{20}\overline{I}(2,3)\\ &+ \frac{35}{2}\overline{L}_{11}\overline{L}_{30} + \sqrt{21}\,\overline{L}_{13}\overline{L}_{30} + 7\sqrt{5}\,\overline{L}_{11}\overline{I}(3,2) + \frac{\sqrt{105}}{3}\overline{L}_{02}\overline{I}(4,1)\Bigg)\end{aligned}$$

$$\begin{aligned}\overline{I}(3,4) =&\overline{L}_{34} - \frac{61}{8}\overline{L}_{30} - \frac{35\sqrt{105}}{12}\overline{L}_{12} - \frac{7\sqrt{5}}{2}\overline{I}(3,2) - \frac{5\sqrt{21}}{6}\overline{I}(1,4)\\ &- \frac{1}{\overline{L}_{00}}\Bigg(\frac{7\sqrt{5}}{2}\overline{L}_{02}\overline{L}_{30} + \overline{L}_{04}\overline{L}_{30} + \frac{9\sqrt{105}}{2}\overline{L}_{11}\overline{L}_{21} + 7\sqrt{5}\,\overline{L}_{13}\overline{L}_{21}\\ &+ \frac{35\sqrt{21}}{6}\overline{L}_{20}\overline{L}_{12} + \frac{35\sqrt{21}}{6}\overline{L}_{02}\overline{L}_{12} + \frac{7\sqrt{105}}{3}\overline{L}_{22}\overline{L}_{12} + 7\overline{L}_{02}\overline{I}(2,3)\\ &+ \frac{35}{2}\overline{L}_{11}\overline{L}_{03} + \sqrt{21}\,\overline{L}_{31}\overline{L}_{03} + 7\sqrt{5}\,\overline{L}_{11}\overline{I}(2,3) + \frac{\sqrt{105}}{3}\overline{L}_{20}\overline{I}(1,4)\Bigg)\end{aligned}$$

$$\begin{aligned}\overline{I}(2,5) =& \overline{L}_{25} - \frac{119\sqrt{33}}{24}\overline{L}_{21} - \frac{3\sqrt{385}}{4}\overline{L}_{03} - \frac{3\sqrt{77}}{2}\overline{I}(2,3) - \frac{\sqrt{5}}{2}\overline{I}(0,5) \\ & - \frac{1}{\overline{L}_{00}}\left(\frac{73\sqrt{165}}{30}\overline{L}_{02}\overline{L}_{21} + \sqrt{33}\,\overline{L}_{04}\overline{L}_{21} + \frac{73\sqrt{33}}{6}\overline{L}_{11}\overline{L}_{12} + 3\sqrt{77}\,\overline{L}_{13}\overline{L}_{12}\right. \\ & + \frac{3\sqrt{77}}{2}\overline{L}_{20}\overline{L}_{03} + \frac{3\sqrt{77}}{2}\overline{L}_{02}\overline{L}_{03} + \frac{3\sqrt{385}}{5}\overline{L}_{22}\overline{L}_{03} + \frac{3\sqrt{385}}{5}\overline{L}_{02}\overline{I}(2,3) \\ & \left. + \sqrt{165}\,\overline{L}_{11}\overline{I}(1,4) + \overline{L}_{20}\overline{I}(0,5)\right)\end{aligned}$$

$$\begin{aligned}\overline{I}(1,6) =& \overline{L}_{16} - \frac{351\sqrt{65}}{40}\overline{L}_{12} - \frac{11\sqrt{13}}{2}\overline{I}(1,4) - \frac{1}{\overline{L}_{00}}\left(\frac{45\sqrt{13}}{2}\overline{L}_{02}\overline{L}_{12}\right. \\ & + \frac{11\sqrt{65}}{5}\overline{L}_{04}\overline{L}_{12} + \frac{109\sqrt{273}}{30}\overline{L}_{11}\overline{L}_{03} + \frac{33\sqrt{13}}{5}\overline{L}_{13}\overline{L}_{03} \\ & \left. + \frac{11\sqrt{65}}{5}\overline{L}_{02}\overline{I}(1,4) + \frac{\sqrt{429}}{3}\overline{L}_{11}\overline{I}(0,5)\right)\end{aligned}$$

$$\begin{aligned}\overline{I}(0,7) =& \overline{L}_{07} - \frac{1727\sqrt{105}}{120}\overline{L}_{03} - \frac{13\sqrt{165}}{6}\overline{I}(0,5) - \frac{1}{\overline{L}_{00}}\left(\frac{1595\sqrt{21}}{42}\overline{L}_{02}\overline{L}_{03}\right. \\ & \left. + \frac{143\sqrt{105}}{35}\overline{L}_{04}\overline{L}_{03} + \frac{13\sqrt{33}}{3}\overline{L}_{02}\overline{I}(0,5)\right)\end{aligned}$$

A2. List of Zernike moment blur invariants up to the sixth order

Zero Order

$$I(0,0) = Z_{0,0}$$

First Order

$$I(1,1) = Z_{1,1}$$

Second Order

$$I(2,2) = Z_{2,2}$$

Third Order

$$\begin{aligned}I(3,1) &= Z_{3,1} - 6I(1,1) - 2I(1,1)\,Z_{2,0}/Z_{0,0} \\ I(3,3) &= Z_{3,3}\end{aligned}$$

Fourth Order

$$\begin{aligned} I(4,2) &= Z_{4,2} - 10I(2,2) - 10I(2,2)\, Z_{2,0}/Z_{0,0} \\ I(4,4) &= Z_{4,4} \end{aligned}$$

Fifth Order

$$\begin{aligned} I(5,1) &= Z_{5,1} - 54I(1,1) - 15I(3,1) - \Big[23I(1,1)\, Z_{2,0} \\ &\quad +3I(1,1)\, Z_{4,0} + 5I(3,1)\, Z_{2,0}\Big]/Z_{0,0} \\ I(5,3) &= Z_{5,3} - 15I(3,3) - 5I(3,3)\, Z_{2,0}/Z_{0,0} \\ I(5,5) &= Z_{5,5} \end{aligned}$$

Sixth Order

$$\begin{aligned} I(6,2) &= Z_{6,2} - 105I(2,2) - 21I(4,2) - \Big[140I(2,2)\, Z_{2,0}/3 \\ &\quad +7I(2,2)\, Z_{4,0} + 7I(4,2)\, Z_{2,0}\Big]/Z_{0,0} \\ I(6,4) &= Z_{6,4} - 21I(4,4) - 7I(4,4)\, Z_{2,0}/Z_{0,0} \\ I(6,6) &= Z_{6,6} \end{aligned}$$

A3. List of combined Zernike moment invariants up to the sixth order

Second Order

$$\begin{aligned} SI(2,0) &= -3\Gamma_f^{-2} I(0,0) + 3\Gamma_f^{-4} I(0,0) + \Gamma_f^{-4} I(2,0) \\ SI(2,2) &= e^{-2\hat{j}\theta_f} \Gamma_f^{-4} I(2,2) \end{aligned}$$

Third Order

$$\begin{aligned} SI(3,1) &= e^{-\hat{j}\theta_f} \left[-4\Gamma_f^{-3} I(1,1) + 4\Gamma_f^{-5} I(1,1) + \Gamma_f^{-5} I(3,1)\right] \\ &= e^{-\hat{j}\theta_f} \Gamma_f^{-5} I(3,1) \\ SI(3,3) &= e^{-2\hat{j}\theta_f} \Gamma_f^{-5} I(3,3) \end{aligned}$$

Fourth Order

$$\begin{aligned}
SI(4,0) &= 5\Gamma_f^{-2} I(0,0) - 15\Gamma_f^{-4} I(0,0) + 10\Gamma_f^{-6} I(0,0) - 5\Gamma_f^{-4} I(2,0) \\
&\quad +5\Gamma_f^{-6} I(2,0) + \Gamma_f^{-6} I(4,0) \\
SI(4,2) &= e^{-2\hat{j}\theta_f}\left[-5\Gamma_f^{-4} I(2,2) + 5\Gamma_f^{-6} I(2,2) + \Gamma_f^{-6} I(4,2)\right] \\
SI(4,4) &= e^{-4\hat{j}\theta_f}\Gamma_f^{-6} I(4,4)
\end{aligned}$$

Fifth Order

$$\begin{aligned}
SI(5,1) &= e^{-\hat{j}\theta_f}\Big[9\Gamma_f^{-3} I(1,1) - 24\Gamma_f^{-5} I(1,1) + 15\Gamma_f^{-7} I(1,1) \\
&\quad -6\Gamma_f^{-5} I(3,1) + \Gamma_f^{-7} I(5,1)\Big] \\
&= e^{-\hat{j}\theta_f}\left[-6\Gamma_f^{-5} I(3,1) + 6\Gamma_f^{-7} I(3,1) + \Gamma_f^{-7} I(5,1)\right] \\
SI(5,3) &= e^{-\hat{j}\theta_f}\left[-6\Gamma_f^{-5} I(3,3) + 6\Gamma_f^{-7} I(3,3) + \Gamma_f^{-7} I(5,3)\right] \\
SI(5,5) &= e^{-5\hat{j}\theta_f}\Gamma_f^{-7} I(5,5)
\end{aligned}$$

Sixth Order

$$\begin{aligned}
SI(6,0) &= -7\Gamma_f^{-2} I(0,0) + 42\Gamma_f^{-4} I(0,0) - 70\Gamma_f^{-6} I(0,0) \\
&\quad +35\Gamma_f^{-8} I(0,0) + 14\Gamma_f^{-4} I(2,0) \\
&= -35\Gamma_f^{-6} I(2,0) + 21\Gamma_f^{-8} I(2,0) - 7\Gamma_f^{-6} I(4,0) \\
&\quad +7\Gamma_f^{-8} I(4,0) + \Gamma_f^{-8} I(6,0) \\
SI(6,2) &= e^{-2\hat{j}\theta_f}\Big[14\Gamma_f^{-4} I(2,2) - 356\Gamma_f^{-6} I(2,2) + 21\Gamma_f^{-8} I(2,2) \\
&\quad -7\Gamma_f^{-6} I(4,2) + 7\Gamma_f^{-8} I(4,2) + \Gamma_f^{-8} I(6,2)\Big] \\
SI(6,4) &= e^{-4\hat{j}\theta_f}\left[-7\Gamma_f^{-6} I(4,4) + 7\Gamma_f^{-8} I(4,4) + \Gamma_f^{-8} I(6,4)\right] \\
SI(6,6) &= e^{-6\hat{j}\theta_f}\Gamma_f^{-8} I(6,6)
\end{aligned}$$

References

[1] F.M. Candocia. Moment relations and blur invariant conditions for finite-extent signals in one, two and N-dimensions. *Pattern Recognition Letters*, 25(4):437–447, 2004.

[2] B. Chen, H. Shu, H. Zhang, G. Coatrieux, L. Luo, and J.L. Coatrieux. Combined invariants to similarity transformation and to blur using orthogonal Zernike moments. *IEEE Transactions on Image Processing*, 20(2):345–360, 2011.

[3] C.W. Chong, P. Raveendran, and R. Mukundan. The scale invariants of pseudo-Zernike moments. *Pattern Analysis and Applications*, 6(3):176–184, 2003.

[4] C.W. Chong, P. Raveendran, and R. Mukundan. Translation and scale invariants of Legendre moments. *Pattern Recognition*, 37(1):119–129, 2004.

[5] S. Derrode and F. Ghorbel. Robust and efficient Fourier–Mellin transform approximations for gray-level image reconstruction and complete invariant description. *Computer Vision and Image Understanding*, 83(1):57–78, 2001.

[6] J. Flusser. On the independence of rotation moment invariants. *Pattern Recognition*, 33(9):1405–1410, 2000.

[7] J. Flusser. On the inverse problem of rotation moment invariants. *Pattern Recognition*, 35(12):3015–3017, 2002.

[8] J. Flusser, J. Boldys, and B. Zitova. Moment forms invariant to rotation and blur in arbitrary number of dimensions. *IEEE Transactions on Pattern Analysis and Machine Intelligence*, 25(2):234–246, 2003.

[9] J. Flusser and T. Suk. Pattern recognition by affine moment invariants. *Pattern Recognition*, 26(1):167–174, 1993.

[10] J. Flusser, T. Suk, and S. Saic. Recognition of blurred images by the method of moments. *IEEE Transactions on Image Processing*, 5(3):533–538, 1996.

[11] J. Flusser, T. Suk, and B. Zitova. *Moments and Moment Invariants in Pattern Recognition*. Wiley, Chichester, United Kingdom, 2009.

[12] J. Flusser and B. Zitova. Combined invariants to linear filtering and rotation. *International Journal of Pattern Recognition and Artificial Intelligence*, 13(8):1123–1136, 1999.

[13] J. Flusser and B. Zitova. Invariants to convolution with circularly symmetric PSF. In *International Conference on Pattern Recognition (ICPR)*, volume 2, pages 11–14, August 2004.

[14] F. Ghorbel, S. Derrode, R. Mezhoud, T. Bannour, and S. Dhahbi. Image reconstruction from a complete set of similarity invariants extracted from complex moments. *Pattern Recognition Letters*, 27(12):1361–1369, 2006.

[15] H. Ji and H. Zhu. Degraded image analysis using Zernike moment invariants. In *IEEE International Conference on Acoustics, Speech and Signal Processing (ICASSP)*, pages 1941–1944, April 2009.

[16] J. Kautsky and J. Flusser. Blur invariants constructed from arbitrary moments. *IEEE Transactions on Image Processing*, 20(12):3606–3611, 2011.

[17] A. Khotanzad and Y.H. Hong. Invariant image recognition by Zernike moments. *IEEE Transactions on Pattern Analysis and Machine Intelligence*, 12(5):489–497, 1990.

[18] J. Liu, D. Li, W. Tao, and L. Yan. An automatic method for generating affine moment invariants. *Pattern Recognition Letters*, 28(16):2295–2304, 2007.

[19] R. Mukundan. Radial Tchebichef invariants for pattern recognition. In *IEEE Region 10 TENCON*, pages 1–6, November 2005.

[20] R. Mukundan and K.R. Ramakrishnan. *Moment Functions in Image Analysis: Theory and Appplications*. World Scientific, Singapore, 1998.

[21] R. Palaniappan, P. Raveendran, and S. Omatu. New invariant moments for non-uniformly scaled images. *Pattern Analysis and Applications*, 3(2):78–87, 2000.
[22] S.C. Pei and C.N. Lin. Image normalization for pattern recognition. *Image and Vision Computing*, 13(10):711–723, 1995.
[23] J.D. Prince. *Computer vision: models, learning and inference*. Cambridge University Press, 2012.
[24] R.J. Prokop and A.P. Reeves. A survey of moment-based techniques for unoccluded object representation and recognition. *CVGIP: Graphical Models and Image Processing*, 54(5):438–460, 1992.
[25] T.H. Reiss. The revised fundamental theorem of moment invariants. *IEEE Transactions on Pattern Analysis and Machine Intelligence*, 13(8):830–834, 1991.
[26] I. Rothe, H. Susse, and K. Voss. The method of normalization to determine invariants. *IEEE Transactions on Pattern Analysis and Machine Intelligence*, 18(4):366–376, 1996.
[27] D. Shen and H.H.S. Ip. Generalized affine invariant image normalization. *IEEE Transactions on Pattern Analysis and Machine Intelligence*, 19(5):431–440, 1997.
[28] Y. Sheng and L. Shen. Orthogonal Fourier-Mellin moments for invariant pattern recognition. *J. Opt. Soc. Am.*, 11(6):1748–1757, 1994.
[29] H. Shu, L. Luo, G. Han, and J.L. Coatrieux. General method to derive the relationship between two sets of Zernike coefficients corresponding to different aperture sizes. *J. Opt. Soc. Am. A*, 23(8):1960–1966, 2006.
[30] H.Z. Shu, J. Zhou, G.N. Han, L.M. Luo, and J.L. Coatrieux. Image reconstruction from limited range projections using orthogonal moments. *Pattern Recognition*, 40(2):670–680, 2007.
[31] T. Suk and J. Flusser. Combined blur and affine moment invariants and their use in pattern recognition. *Pattern Recognition*, 36(12):2895–2907, 2003.
[32] T. Suk and J. Flusser. Graph method for generating affine moment invariants. In *International Conference on Pattern Recognition (ICPR)*, volume 2, pages 192–195, 2004.
[33] T. Suk and J. Flusser. Affine normalization of symmetric objects. In *Advanced Concepts for Intelligent Vision Systems*, volume 3708 of *LNCS*, pages 100–107. 2005.
[34] R. Szeliski. *Computer vision: algorithms and applications*. Springer, 2010.
[35] C.H. Teh and R.T. Chin. On image analysis by the methods of moments. *IEEE Transactions on Pattern Analysis and Machine Intelligence*, 10(4):496–513, 1988.
[36] B. Xiao, J.F. Ma, and X. Wang. Image analysis by Bessel–Fourier moments. *Pattern Recognition*, 43(8):2620–2629, 2010.
[37] H. Zhang, H. Shu, G. Coatrieux, J. Zhu, Q.M.J. Wu, Y. Zhang, H. Zhu, and L. Luo. Affine Legendre moment invariants for image watermarking robust to geometric distortions. *IEEE Transactions on Image Processing*, 20(8):2189–2199, 2011.
[38] H. Zhang, H. Shu, G.N. Han, G. Coatrieux, L. Luo, and J.L. Coatrieux. Blurred image recognition by Legendre moment invariants. *IEEE Transactions on Image Processing*, 19(3):596–611, 2010.
[39] H. Zhang, H.Z. Shu, P. Haigron, B.S. Li, and L.M. Luo. Construction of a complete set of orthogonal Fourier–Mellin moment invariants for pattern recognition

applications. *Image and Vision Computing*, 28(1):38–44, 2010.

[40] H. Zhang and Q.M.J. Wu. Pattern recognition by affine Legendre moment invariants. In *IEEE International Conference on Image Processing (ICIP)*, pages 797–800, 2011.

[41] Y. Zhang, C. Wen, Y. Zhang, and Y.C. Soh. On the choice of consistent canonical form during moment normalization. *Pattern Recognition Letters*, 24(16):3205–3215, 2003.

[42] H. Zhu, M. Liu, H. Ji, and Y. Li. Combined invariants to blur and rotation using Zernike moment descriptors. *Pattern Analysis and Applications*, 13(3):309–319, 2010.

[43] H. Zhu, H. Shu, T. Xia, L. Luo, and J.L. Coatrieux. Translation and scale invariants of Tchebichef moments. *Pattern Recognition*, 40(9):2530–2542, 2007.